Metallophysics and Advanced Technologies
Металофіз. новітні технол.
Metallofiz. Noveishie Tekhnol.
2019, vol. 41, No. 11, pp. 1433–1454
https://doi.org/10.15407/mfint.41.11.1433
Reprints available directly from the publisher

CRYSTAL-LATTICE DEFECTS

PACS numbers: 02.30.Uu, 66.30.Dn, 68.35.Ct, 68.35.Fx, 81.10.Aj

Coupled Morphological Stability of the Multiple Phase Boundaries: Oxides in an Oxygen Potential Gradient. I. Single Oxide Layer

Petro O. Mchedlov-Petrosyan and Manfred Martin*

National Science Center 'Kharkiv Institute of Physics and Technology', N.A.S. of Ukraine, A. I. Akhiezer Institute for Theoretical Physics, 1 Akademichna Str., UA-61108 Kharkiv, Ukraine
**RWTH Aachen University, Institute of Physical Chemistry, 55 Templergraben, 52056 Aachen, Germany*

The morphological stability of interphase boundaries is a challenging problem, both from a mathematical and a physical point of view. In materials that are exposed to thermodynamic potential gradients, *i.e.*, gradients of chemical potentials, electrical potential, temperature, or pressure, transport processes of the mobile components occur. These transport processes may cause morphological instabilities of the material surfaces and interfaces. In this paper, a comprehensive formal treatment of the coupled morphological stability of multiple phase boundaries will be given for oxides that are exposed to an oxygen potential gradient. In Part I, we study a single oxide layer, that is the morphological stability of two-boundaries; two oxide layers, *i.e.* the case of three boundaries will be treated in the Part II. To explore the stability of diffusionally interacting boundaries an original, new method is applied. Based on an integral transformation of a special kind, this method reveals the evolution of the multiple boundaries' perturbations without solving the diffusional problem inside the layer. The study of the morphological stability of the stationary moving boundaries is thereby reduced to the exploration of the singular points (in the complex plane) of the corresponding integrands.

Key words: morphological stability, multi-phase system, diffusional mass

Corresponding author: Petro Otarovych Mchedlov-Petrosyan
E-mail: peter.mchedlov@free.fr

Citation: Petro O. Mchedlov-Petrosyan and Manfred Martin, Coupled Morphological Stability of the Multiple Phase Boundaries: Oxides in an Oxygen Potential Gradient. I. Single Oxide Layer, *Metallofiz. Noveishie Tekhnol.*, **41**, No. 11: 1433–1454 (2019), DOI: 10.15407/mfint.41.11.1433.

transport, integral transform.

Морфологічна стійкість міжфазних границь являє собою серйозну проблему як з математичної, так і з фізичної точки зору. У матеріалах, підданих дії градієнтів термодинамічних потенціалів, тобто градієнтів хімічних потенціалів, електричних потенціалів, температури або тиску, виникають процеси переносу мобільних компонентів. Ці процеси можуть викликати морфологічні нестійкості поверхонь і міжфазних границь. У цій статті для оксидів, що знаходяться під дією градієнта хімічного потенціалу кисню, дається детальне теоретичне дослідження взаємозалежної морфологічної стійкості. У частині I ми досліджуємо один оксидний шар, тобто морфологічну стійкість двох границь; випадок двох оксидних шарів, тобто трьох границь, буде розглянутий у частині II. Для дослідження взаємозалежної стійкості дифузійно взаємодіючих границь використовується новий математичний метод, заснований на спеціальному інтегральному перетворенні. Цей метод дозволяє виявляти еволюцію збурень множинних границь без вирішення дифузійної задачі усередині шару. Тим самим вивчення морфологічної стійкості границь, що стаціонарно рухаються, зводиться до дослідження сингулярностей (у комплексній площині) підінтегральних виразів певних інтегралів.

Ключові слова: морфологічна стійкість, багатофазні системи, дифузійне масоперенесення, інтегральне перетворення.

Морфологическая устойчивость межфазных границ представляет собой серьёзную проблему как с математической, так и с физической точки зрения. В материалах, подверженных действию градиентов термодинамических потенциалов, т.е. градиентов химических потенциалов, электрических потенциалов, температуры или давления, возникают процессы переноса мобильных компонентов. Эти процессы могут вызывать морфологические неустойчивости поверхностей и межфазных границ. В этой статье для оксидов, находящихся под действием градиента химического потенциала кислорода, даётся детальное теоретическое исследование взаимосвязанной морфологической устойчивости. В части I мы исследуем один оксидный слой, т.е. морфологическую устойчивость двух границ; случай двух оксидных слоёв, т.е. трёх границ, будет рассмотрен в части II. Для исследования взаимосвязанной устойчивости диффузионно взаимодействующих границ используется новый математический метод, основанный на специальном интегральном преобразовании. Этот метод позволяет выявлять эволюцию возмущений множественных границ без решения диффузионной задачи внутри слоя. Тем самым изучение морфологической устойчивости стационарно движущихся границ сводится к исследованию сингулярностей (в комплексной плоскости) подинтегральных выражений определённых интегралов.

Ключевые слова: морфологическая устойчивость, многофазные системы, диффузионный массоперенос, интегральное преобразование.

(Received May 5, 2019)

1. INTRODUCTION

In many applications originally homogeneous materials are exposed to thermodynamic potential gradients, which can be gradients of temperature, chemical potential of one or more elements, electrical potential or uniaxial pressure. Well known examples are tarnishing layers on metallic materials [1, 2] which act as corrosion protection, thermal barrier coatings [3] acting as heat shield, solid electrolytes in fuel cells [4], or gas separation membranes [5]. The applied gradients act as a generalized thermodynamic forces, and induce directed fluxes of the mobile components. These fluxes may lead to a practically very important degradation phenomenon of the materials: The original morphology of the material surfaces might become unstable and a new surface morphology might be established (morphological instability) [6]. In addition to the practical implications, this moving-boundary problem is mathematically challenging. To explore the stability of diffusionally interacting boundaries, in this paper an original, new method is applied. Based on an integral transformation of a special kind, this method reveals the evolution of the multiple boundaries' perturbations without solving the diffusional problem inside the layer. The study of the morphological stability of the stationary moving boundaries is thereby reduced to exploration of the singular points (in the complex plane) of the corresponding integrands.

The class of materials considered here will be limited to oxides. Examples are Al_2O_3 tarnishing layers on metallic alloys [1], ZrO_2-layers in thermal barrier coatings [3], Y_2O_3-doped ZrO_2 (YSZ) being the solid electrolyte in solid oxide fuel cells (SOFC) and solid oxide electrolyzer cells (SOEC), (La, Sr)MnO_{3-d} being the cathode material in (SOFCs) [4], or (La, Sr)CrO_{3-d} in oxygen separation membranes [5]. Recently, very thin oxide films, *e.g.* $SrTiO_3$ or GaO_x have found increased interest due to their ability for resistive switching [7, 8]. In all of these examples, oxygen potential gradients appear across the oxide layer, either directly applied externally or as a result of another applied gradient.

In this paper we consider a semiconducting binary oxide $A_{1-\delta}O$ where oxygen is practically immobile, while cations A are mobile *via* cation vacancies V (with fraction $\delta << 1$). Examples are the binary transition metal oxides (A = Ni, Co, Fe, Mn). In Part I of this paper, the morphological stability of $A_{1-\delta}O$ exposed to an external oxygen potential gradient will be investigated in an exact way and will be compared to our earlier, approximate solution [9].

In a nonstoichiometric binary transition metal oxide $A_{1-\delta}O$ the concentration of cation vacancies increases with increasing oxygen partial pressure in the surrounding gas. If such an oxide is chemically reduced by lowering the oxygen partial pressure, cation vacancies V, and electron holes $h^{\bullet}$ diffuse to the crystal surface, where reduction of the ox-

ide takes place:

$$O^{2-} + V + 2h^{\bullet} \rightarrow \frac{1}{2}O_2(g). \quad (1)$$

This reduction process corresponds to the arrival of a vacancy and two electron holes at the surface and the release of oxygen from the crystal. Thus a structural unit composed of a cation vacancy and an anion, is removed from the crystal while the number of cations is conserved. The crystal surface acts as vacancy sink until the new equilibrium state is reached. In contrast to this non-stationary situation, a stationary non-equilibrium state can be established by exposing an oxide layer with two parallel surfaces to a gradient of the oxygen partial pressure, resulting in reduction at the low oxygen potential side and oxidation (the reversal of the above reaction (1)) at the high oxygen potential side (Fig. 1).

After a transient time, a stationary flux of vacancies and a corresponding flux of A-ions in the opposite direction occur, which are fed by the surface reaction (1) and the reverse of it. As a result of this 'vacancy wind' both crystal surfaces move (relative to the immobile oxygen sublattice) towards the side of higher partial pressure.

The corresponding one-dimensional diffusion problem was solved under the following assumptions [9]: i) the crystal surfaces are planar. ii) The chemical diffusion coefficient D is constant. iii) Local equilibrium is established at the boundaries, *i.e.* phase boundary reaction kinetics is very fast compared to bulk diffusion. The stationary solution was obtained by transforming the diffusion equation for the vacancies (or the cations A) and the mass balances at the oxide/gas boundaries to

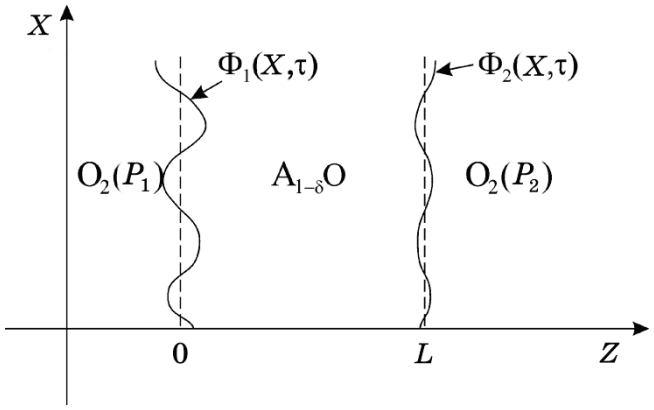

Fig. 1. Schematic presentation of an oxide $A_{1-\delta}O$ exposed to an oxygen potential gradient. P_1 and P_2 ($>P_1$) are the corresponding oxygen partial pressures in the gas phases. Dashed lines represent planar oxide surfaces, solid lines perturbed surfaces. L is the width of the oxide layer.

a moving reference frame, $0 \le z \le L$ (L is the sample thickness), in which both surfaces are at rest.

Now, the question about the morphological stability of the surfaces of such a moving oxide layer naturally arises. Remarkably, despite the huge amount of publications on the subject of morphological stability, to the best of our knowledge the stability of two or more surfaces coupled by the diffusional mass transfer was not studied. In the present work the problem of linear stability of such surfaces is treated analytically. For two coupled surfaces (single layer) the results are exact; they are then compared to the results of a quasi-stationary approximation, which is shown to be quite precise. The coupled stability of three surfaces (two layers of different oxides of the same metal) will be considered in the Part II of this paper.

2. SETTING OF THE PROBLEM

In Ref. [9] we found that the surfaces (1) and (2) exhibit different morphological stabilities. While surface (1) was morphologically unstable, surface (2) was morphologically stable. These experimental results were supported by means of a linear stability analysis of each surface without any diffusional coupling of the surfaces. In the present work, this problem is generalized by exploring the morphological stability of two diffusionally interacting surfaces.

It is worth mentioning that from the formal point the result of [9] may look paradoxical: if the interaction of the boundaries is taken into account the perturbations of the boundaries are governed by a coupled linear equation system; a linear system could be either stable or unstable as a whole; so formally both boundaries with necessity should be either stable or unstable. Below we see how this paradox is resolved in a very clear and physical way. To explore the stability of diffusionally interacting boundaries the method developed in [10, 11] is applied. The problem is solved analytically; the detailed descriptions of the (necessary) quite lengthy calculations can be found in the Appendixes.

For convenience we reiterate the problem setting from [9] (the present notations are slightly different). In the moving reference frame, moving with a constant velocity V relative to the immobile oxygen sublattice (identical to the laboratory frame, see Fig. 1) the governing equation takes the form

$$\frac{\partial C}{\partial \tau} - V\frac{\partial C}{\partial Z} - D\left(\frac{\partial^2 C}{\partial X^2} + \frac{\partial^2 C}{\partial Z^2}\right) = 0, \qquad (2)$$

where $C = \delta/\omega$ is the vacancy concentration, ω the molar volume of the oxide AO, D is the chemical diffusion coefficient (both of which are presumed to be constant that is independent on δ), X and Z the spatial

coordinates (see Fig. 1), and τ the time.

Looking for small deviations $u(X, Z, \tau)$ from the stationary solution $C_s(Z)$ corresponding to constant width L of the oxide layer

$$C = C_s(Z) + u(X, Z, \tau) \tag{3}$$

and slightly non planar, non-stationary boundaries (see Fig. 1)

$$Z_1(X, \tau) = 0 + \Phi_1(X, \tau), \quad Z_2(X, \tau) = L + \Phi_2(X, \tau), \tag{4}$$

the (equilibrium) boundary conditions are

$$C_s\big|_{Z=0} + u\big|_{Z=0} + \left.\frac{\partial C_s}{\partial Z}\right|_{Z=0} \Phi_1(X, \tau) = C_1\left(1 - \tilde{\Gamma}_1 \frac{\partial^2 \Phi_1}{\partial X^2}\right), \tag{5}$$

$$C_s\big|_{Z=L} + u\big|_{Z=L} + \left.\frac{\partial C_s}{\partial Z}\right|_{Z=L} \Phi_2(X, \tau) = C_2\left(1 + \tilde{\Gamma}_2 \frac{\partial^2 \Phi_2}{\partial X^2}\right), \tag{6}$$

where $\tilde{\Gamma}_{1,2}$ are the capillary lengths. The mass balance equations at both boundaries are

$$V + \dot{\Phi}_1(X, \tau) = \frac{\omega}{1 - \delta_1} D\left(\left.\frac{\partial C_s}{\partial Z}\right|_{Z=0} + \left.\frac{\partial u}{\partial Z}\right|_{Z=0} + \left.\frac{\partial^2 C_s}{\partial Z^2}\right|_{Z=0} \Phi_1(X, \tau)\right), \tag{7}$$

$$V + \dot{\Phi}_2(X, \tau) = \frac{\omega}{1 - \delta_2} D\left(\left.\frac{\partial C_s}{\partial Z}\right|_{Z=L} + \left.\frac{\partial u}{\partial Z}\right|_{Z=L} + \left.\frac{\partial^2 C_s}{\partial Z^2}\right|_{Z=L} \Phi_2(X, \tau)\right), \tag{8}$$

where $\delta_i, i = 1, 2$ are the deviations from stoichiometry at the corresponding boundaries. If we look for the stationary ('zero order') solution, which is only Z-dependent, both the equation (2) and the boundary conditions (5)–(8) simplify essentially. The solution of this system is given in Appendix 1; the corresponding stationary values [9] of the layer width L and the velocity V are given by Eqs. (90) and (91).

3. STABILITY ANALYSIS FOR THE SINGLE OXIDE LAYER

We consider the single oxide layer, *i.e.* is the coupled morphological stability of two gas/solid interfaces (see Fig. 1). The governing equation and boundary conditions for the first order perturbations are (see (2)–(8))

$$\frac{1}{D}\frac{\partial u}{\partial \tau} = \frac{V}{D}\frac{\partial u}{\partial Z} + \frac{\partial^2 u}{\partial X^2} + \frac{\partial^2 u}{\partial Z^2}, \tag{9}$$

$$u\Big|_{Z=0} + \frac{V}{D}\frac{1-\delta_1}{\omega}\Phi_1(X,\tau) + C_1\tilde{\Gamma}_1\frac{\partial^2\Phi_1}{\partial X^2} = 0, \tag{10}$$

$$u\Big|_{Z=L} + \frac{V}{D}\frac{1-\delta_2}{\omega}\Phi_2(X,\tau) - C_2\tilde{\Gamma}_2\frac{\partial^2\Phi_2}{\partial X^2} = 0, \tag{11}$$

$$\frac{1}{D}\frac{\partial\Phi_1}{\partial\tau} = \frac{\omega}{1-\delta_1}\frac{\partial u}{\partial Z}\Big|_{Z=0} - \left(\frac{V}{D}\right)^2\Phi_1(X,\tau), \tag{12}$$

$$\frac{1}{D}\frac{\partial\Phi_2}{\partial\tau} = \frac{\omega}{1-\delta_2}\frac{\partial u}{\partial Z}\Big|_{Z=L} - \left(\frac{V}{D}\right)^2\Phi_2(X,\tau), \tag{13}$$

where we have used the expressions (92), (93) for the values of the derivatives $\left.\frac{\partial C_s}{\partial Z}\right|_{Z=0}$, $\left.\frac{\partial^2 C_s}{\partial Z^2}\right|_{Z=0}$ and $\left.\frac{\partial C_s}{\partial Z}\right|_{Z=L}$, $\left.\frac{\partial^2 C_s}{\partial Z^2}\right|_{Z=L}$, see Appendix 1. Taking the stationary width L of the layer as the length scale and, correspondingly rescaling all other lengths $Z/L = z$, $X/L = x$, $\Phi_i / L = \varphi_i$, $\tilde{\Gamma}_i / L = \Gamma_i$, and time $\tau / \left(L^2/D\right) = t$, and measuring u in molar fractions $\omega u = \tilde{u}$ we are led to the dimensionless system for the concentration's perturbation field

$$\frac{\partial\tilde{u}}{\partial t} = 2\xi\frac{\partial\tilde{u}}{\partial z} + \frac{\partial^2\tilde{u}}{\partial x^2} + \frac{\partial^2\tilde{u}}{\partial z^2}, \tag{14}$$

where

$$\xi = \frac{VL}{2D} = \frac{1}{2}\ln\frac{1-\delta_1}{1-\delta_2}. \tag{15}$$

The boundary conditions at the positions of the planar boundaries, $z = 0$ and $z = 1$, are

$$\tilde{u}\Big|_{z=0} + 2\xi(1-\delta_1)\varphi_1(x,t) + \delta_1\Gamma_1\frac{\partial^2\varphi_1}{\partial x^2} = 0, \tag{16}$$

$$\tilde{u}\Big|_{z=1} + 2\xi(1-\delta_2)\varphi_2(x,t) - \delta_2\Gamma_2\frac{\partial^2\varphi_2}{\partial x^2} = 0, \tag{17}$$

$$\frac{\partial\varphi_1}{\partial t} = \frac{1}{1-\delta_1}\frac{\partial\tilde{u}}{\partial z}\Big|_{z=0} - 4\xi^2\varphi_1(x,t), \tag{18}$$

$$\frac{\partial\varphi_2}{\partial t} = \frac{1}{1-\delta_2}\frac{\partial\tilde{u}}{\partial z}\Big|_{z=1} - 4\xi^2\varphi_2(x,t). \tag{19}$$

Introducing the Fourier transforms

$$\varphi_j(x,t) = \frac{1}{\sqrt{2\pi}} \int_{-\infty}^{\infty} dk \exp(ikx)\overline{\varphi}_j(k,t),\ j = 1, 2, \tag{20}$$

$$\tilde{u}(x,z,t) = \frac{1}{\sqrt{2\pi}} \int_{-\infty}^{\infty} dk \exp(ikx)\overline{u}(k,z,t) \tag{21}$$

we obtain from (14) and (16)–(19)

$$\frac{\partial \overline{u}}{\partial t} = 2\xi \frac{\partial \overline{u}}{\partial z} + \frac{\partial^2 \overline{u}}{\partial z^2} - k^2 \overline{u}, \tag{22}$$

$$\overline{u}\Big|_{z=0} + 2\xi(1-\delta_1)\overline{\varphi}_1 - \delta_1 \Gamma_1 k^2 \overline{\varphi}_1 = 0, \tag{23}$$

$$\overline{u}\Big|_{z=1} + 2\xi(1-\delta_2)\overline{\varphi}_2 + \delta_2 \Gamma_2 k^2 \overline{\varphi}_2 = 0, \tag{24}$$

$$\frac{\partial \overline{\varphi}_1}{\partial t} = \frac{1}{1-\delta_1} \frac{\partial \overline{u}}{\partial z}\Big|_{z=0} - 4\xi^2 \overline{\varphi}_1, \tag{25}$$

$$\frac{\partial \overline{\varphi}_2}{\partial t} = \frac{1}{1-\delta_2} \frac{\partial \overline{u}}{\partial z}\Big|_{z=1} - 4\xi^2 \overline{\varphi}_2. \tag{26}$$

The method [10, 11] to be applied below essentially uses the asymptotical (in time) finiteness of $\overline{u}$, $\overline{\varphi}_1$, and $\overline{\varphi}_2$. Therefore, to take into account the possible instability (which we are looking for) the new variables are introduced:

$$w = \overline{u} \exp(-\eta t), \tag{27}$$

$$\gamma_i = \overline{\varphi}_i \exp(-\eta t),\ \ i = 1, 2, \tag{28}$$

where the constant $\eta > 0$ at the moment remains undetermined. In terms of these new variables (22)–(26) become

$$\frac{\partial w}{\partial t} = 2\xi \frac{\partial w}{\partial z} + \frac{\partial^2 w}{\partial z^2} - (k^2 + \eta) w, \tag{29}$$

$$w\Big|_{z=0} + \left[2\xi(1-\delta_1) - \delta_1 \Gamma_1 k^2\right] \gamma_1(k,t) = 0, \tag{30}$$

$$w\Big|_{z=1} + \left[2\xi(1-\delta_2) + \delta_2 \Gamma_2 k^2\right] \gamma_2(k,t) = 0, \tag{31}$$

$$\frac{\partial \gamma_1}{\partial t} = \frac{1}{1-\delta_1} \frac{\partial w}{\partial z}\Big|_{z=0} - (4\xi^2 + \eta)\gamma_1, \tag{32}$$

$$\frac{\partial \gamma_2}{\partial t} = \frac{1}{1-\delta_2} \frac{\partial w}{\partial z}\Big|_{z=1} - (4\xi^2 + \eta)\gamma_2. \tag{33}$$

The term $\eta \cdot \omega$ in (29) may be considered physically as some kind of fictitious 'dissipation', which may be adjusted to compensate the possible instability. Now the method [10, 11] is applied. First we perform the integral transformations of (29) using as a kernel functions

$$K_n = \exp(\nu_n z), \quad n = 1, 2, \tag{34}$$

where

$$\nu_{1,2} = \xi \pm \sqrt{\xi^2 + k^2 + \eta + p}, \quad p > 0, \tag{35}$$

i.e. is we introduce

$$I_n(k, p, t) = \int_0^1 w(k, z, t) \exp(\nu_n z) dz, \quad n = 1, 2. \tag{36}$$

This yields two ordinary differential equations for I_n

$$\frac{\partial I_n}{\partial t} = pI_n + \Phi_n, \; n = 1, 2, \tag{37}$$

where

$$\Phi_n = (2\xi - \nu_n)\left[w\big|_{z=1} \exp(\nu_n) - w\big|_{z=0} \right] + \frac{\partial w}{\partial z}\bigg|_{z=1} \exp(\nu_n) - \frac{\partial w}{\partial z}\bigg|_{z=0}. \tag{38}$$

Solving (37) we obtain

$$I_n(p, k, t) \exp(-pt) = \int_0^t \Phi_n \exp(-pq) dq + I_{n0}, \quad n = 1, 2, \tag{39}$$

$$I_{n0} = \int_0^1 \bar{u}(k, z, 0) \exp(\nu_n z) dz, \quad n = 1, 2, \tag{40}$$

where $\bar{u}(k, z, 0)$ is the Fourier transform (see (21)) of initial deviations of the concentration from the stationary solution inside the layer.

Even if the stationary solution appears to be unstable, that is the boundary perturbations φ_i are increasing with time, selecting η (see (27), (28)), we can always 'shift' w, γ_i to the stability threshold. At the threshold I_n are (see (36)) limited for $t \to \infty$. Taking this limit on both sides of (39), we get

$$0 = \int_0^\infty \Phi_n \exp(-pq) dq + I_{n0}(k, p, 0), \quad n = 1, 2. \tag{41}$$

Using the boundary conditions (30)–(33), w and its derivatives could be eliminated from (38), and Φ_n could be expressed *via* γ_i and $\partial \gamma_i / \partial t$ only, this yields a system of two integral equations for γ_1 and γ_2. The method, described above, was developed in [10, 11] on the basis of an approach designed by Chekmaryova [13] for the solution of the one-dimensional moving boundary problems for diffusion equations. While

for the moving boundary problems the integral equations (the analogue of (41)) are highly nonlinear, (41) is a linear one. Even more, for the present case it turns out to be a linear equation for the Laplace transforms of γ_1, γ_2. Denoting the Laplace transforms of γ_i as $\bar{\gamma}_i$, we arrive at the following algebraic system of equations for $\bar{\gamma}_i$

$$\begin{aligned}
&\exp(\nu_1)\left[(1-\delta_2)(2\xi\nu_1 + p + \eta) - \nu_2\delta_2\Gamma_2 k^2\right]\bar{\gamma}_2 - \\
&- \left[(1-\delta_1)(2\xi\nu_1 + p + \eta) + \nu_2\delta_1\Gamma_1 k^2\right]\bar{\gamma}_1 = \qquad (42)\\
&= -I_{10}(k, p, 0) + (1-\delta_2)\exp(\nu_1)\gamma_2(k, 0) - (1-\delta_1)\gamma_1(k, 0),\\
&\exp(\nu_2)\left[(1-\delta_2)(2\xi\nu_2 + p + \eta) - \nu_1\delta_2\Gamma_2 k^2\right]\bar{\gamma}_2 - \\
&- \left[(1-\delta_1)(2\xi\nu_2 + p + \eta) + \nu_1\delta_1\Gamma_1 k^2\right]\bar{\gamma}_1 = \qquad (43)\\
&= -I_{20}(k, p, 0) + (1-\delta_2)\exp(\nu_2)\gamma_2(k, 0) - (1-\delta_1)\gamma_1(k, 0),
\end{aligned}$$

where $\gamma_i(k, 0) = \bar{\varphi}_i(k, 0)$, that is initial values of the k-th Fourier mode of the boundaries' perturbations. Introducing notations

$$\bar{\Gamma}_i = \frac{\delta_i\Gamma_i}{1-\delta_i},\ i = 1, 2, \quad \bar{I}_{10} = I_{10}\frac{1}{1-\delta_1},\ \bar{I}_{20} = \frac{1}{1-\delta_2}I_{20}, \qquad (44)$$

and taking into account (see (15) and (35))

$$\frac{1-\delta^{(2)}}{1-\delta^{(1)}} = \exp(-2\xi),\ \ \nu_1 + \nu_2 = 2\xi$$

we rewrite (42), (43), as

$$\begin{aligned}
&\exp(-\nu_2)\left[(2\xi\nu_1 + p + \eta) - \nu_2\bar{\Gamma}_2 k^2\right]\bar{\gamma}_2 - \\
&- \left[(2\xi\nu_1 + p + \eta) + \nu_2\bar{\Gamma}_1 k^2\right]\bar{\gamma}_1 = \qquad (45)\\
&= -\bar{I}_{10}(k, p, 0) + \exp(-\nu_2)\gamma_2(k, 0) - \gamma_1(k, 0),\\
&\exp(-\nu_1)\left[(2\xi\nu_2 + p + \eta) - \nu_1\bar{\Gamma}_2 k^2\right]\bar{\gamma}_2 - \\
&- \left[(2\xi\nu_2 + p + \eta) + \nu_1\bar{\Gamma}_1 k^2\right]\bar{\gamma}_1 = \qquad (46)\\
&= -\bar{I}_{20}(k, p, 0) + \exp(-\nu_1)\gamma_2(k, 0) - \gamma_1(k, 0).
\end{aligned}$$

Zero Surface Tension Case. In the present work we are mainly targeting the effect of the diffusional interaction of the moving boundaries on their morphological stability. Both renormalized capillary lengths $\bar{\Gamma}_i$ are quite small (see (44): $\Gamma_i = \frac{\tilde{\Gamma}_i}{L} \sim 10^{-6}$, $\frac{\delta_i}{1-\delta_i} \sim 10^{-2}$, or

less). That is, the influence of surface tension may be essential only for the perturbations with the wave length less than $L \cdot 10^{-4}$ [9]. So we may first set for simplicity $\overline{\Gamma}_i = 0$, postponing the discussion of the nonzero Γ_i to a future work. We also do not consider the effect of initial perturbations of the concentration field inside the layer, taking $\overline{I}_{10} = \overline{I}_{20} = 0$. It was shown in [10] that for rather weak assumptions about the initial perturbations of the concentration field inside the layer (expandability in a converging Taylor series) their influence on the boundaries' instability is negligible. Then the system (45), (46) takes the form:

$$(2\xi\nu_1 + p + \eta)\left[\exp(-\nu_2)\bar{\gamma}_2 - \bar{\gamma}_1\right] = \\ = \exp(-\nu_2)\gamma_2(k,0) - \gamma_1(k,0), \tag{47}$$

$$(2\xi\nu_2 + p + \eta)\left[\exp(-\nu_1)\bar{\gamma}_2 - \bar{\gamma}_1\right] = \\ = \exp(-\nu_1)\gamma_2(k,0) - \gamma_1(k,0). \tag{48}$$

Solving system (47), (48) for $\bar{\gamma}_i$, we obtain

$$\bar{\gamma}_1 = \bar{F}_{11}\gamma_1(k,0) + \bar{F}_{12}\gamma_2(k,0), \tag{49}$$

$$\bar{\gamma}_2 = \bar{F}_{21}\gamma_1(k,0) + \bar{F}_{22}\gamma_2(k,0), \tag{50}$$

where the functions $\bar{F}_{ij}$ are:

$$\bar{F}_{11} = \frac{1}{1 - \exp(\nu_2 - \nu_1)}\left[\frac{1}{2\xi\nu_2 + p + \eta} - \frac{\exp(\nu_2 - \nu_1)}{2\xi\nu_1 + p + \eta}\right], \tag{51}$$

$$\bar{F}_{12} = \frac{\exp(-\nu_1)}{1 - \exp(\nu_2 - \nu_1)}\left[\frac{1}{2\xi\nu_1 + p + \eta} - \frac{1}{2\xi\nu_2 + p + \eta}\right], \tag{52}$$

$$\bar{F}_{21} = \frac{\exp(\nu_2)}{1 - \exp(\nu_2 - \nu_1)}\left[\frac{1}{2\xi\nu_2 + p + \eta} - \frac{1}{2\xi\nu_1 + p + \eta}\right], \tag{53}$$

$$\bar{F}_{22} = \frac{1}{1 - \exp(\nu_2 - \nu_1)}\left[\frac{1}{2\xi\nu_1 + p + \eta} - \frac{\exp(\nu_2 - \nu_1)}{2\xi\nu_2 + p + \eta}\right]. \tag{54}$$

Performing the inverse Laplace transform, one obtains the exact (fully time-dependent) expressions for the evolution of the boundary perturbations:

$$\gamma_1(k,t) = F_{11}\gamma_1(k,0) + F_{12}\gamma_2(k,0), \tag{55}$$

$$\gamma_2(k,t) = F_{21}\gamma_1(k,0) + F_{22}\gamma_2(k,0). \tag{56}$$

Here

$$F_{ij} = \frac{1}{2\pi i} \int_{a-i\infty}^{a+i\infty} \widehat{F}_{ij}(p,k) \exp(pt) dp. \tag{57}$$

It is evident from (55), (56) that the F_{11} and F_{22} exhibit the 'self-action' of the reducing and oxidizing boundaries, respectively, that is the evolution of their own initial perturbations. On the other hand, the F_{12} and F_{21} reveal the 'cross-action', that is the influence of the initial perturbation of the oxidizing boundary on the evolution of the reducing boundary and *vice versa*.

Of cause, this result may be obtained by the complete solution of the problem (29)–(33) *via* the Laplace transformation. However we succeeded in obtaining $\gamma_i(k, t)$ only, without solving the problem completely. With increasing number of the boundaries, and/or of the components, this difference becomes increasingly important. Even more, to explore stability we do not need the full solutions for $\gamma_i(k, t)$. It is sufficient to detect the fastest growing modes only, which, in turn are determined by the singularities of the corresponding integrands in (57). It is convenient to introduce the new variable y:

$$y = \xi^2 + k^2 + \eta + p. \tag{58}$$

Then $\nu_1 = \xi + \sqrt{y}$, $\nu_2 = \xi - \sqrt{y}$, see Eq. (35), $p = y - \xi^2 - k^2 - \eta$ and (51)–(54) may be rewritten as

$$\widehat{F}_{11} = \frac{1}{1 - \exp(-2\sqrt{y})} \left[\frac{1}{(\sqrt{y} - \xi - k)(\sqrt{y} - \xi + k)} - \right.$$
$$\left. - \frac{\exp(-2\sqrt{y})}{(\sqrt{y} + \xi - k)(\sqrt{y} + \xi + k)} \right], \tag{59}$$

$$\widehat{F}_{12} = \frac{\exp(-\xi - \sqrt{y})}{1 - \exp(-2\sqrt{y})} \left[\frac{1}{(\sqrt{y} + \xi - k)(\sqrt{y} + \xi + k)} - \right.$$
$$\left. - \frac{1}{(\sqrt{y} - \xi - k)(\sqrt{y} - \xi + k)} \right], \tag{60}$$

$$\widehat{F}_{21} = \frac{\exp(\xi - \sqrt{y})}{1 - \exp(-2\sqrt{y})} \left[\frac{1}{(\sqrt{y} - \xi - k)(\sqrt{y} - \xi + k)} - \right.$$
$$\left. - \frac{1}{(\sqrt{y} + \xi - k)(\sqrt{y} + \xi + k)} \right], \tag{61}$$

$$\widehat{F}_{22} = \frac{1}{1-\exp(-2\sqrt{y})}\left[\frac{1}{(\sqrt{y}+\xi-k)(\sqrt{y}+\xi+k)} - \right.$$
$$\left. - \frac{\exp(-2\sqrt{y})}{(\sqrt{y}-\xi-k)(\sqrt{y}-\xi+k)}\right]. \tag{62}$$

Making use of (57) we get

$$F_{lr} = \frac{1}{2\pi i}\exp\left\{-(\xi^2+k^2+\eta)t\right\}\left[J_{lr}^{(1)} - J_{lr}^{(2)}\right],\ l, r = 1, 2. \tag{63}$$

From the eight integrals $J_{lr}^{(m)}$, $l, r, m = 1, 2$ we show here only $J_{11}^{(1)}$ as an example; all $J_{lr}^{(m)}$, are given in the Appendix 2.

$$J_{11}^{(1)} = \int_{a-i\infty}^{a+i\infty} \frac{(\sqrt{y}+\xi+k)\exp(yt)}{\left(1-\exp(-2\sqrt{y})\right)\left(y-(k+\xi)^2\right)\left(\sqrt{y}-\xi+k\right)}\,dy. \tag{64}$$

The integrand of each $J_{lr}^{(m)}$, has a branching point at $y = 0$ and two poles; only the pole with the maximal real part is of interest. Thus the 8 integrals $J_{lr}^{(m)}$ are segregated into two sets: those with maximal real part of the pole $(k+\xi)^2$ and those with maximal real part of the pole $(k-\xi)^2$. The former set includes $J_{11}^{(1)}$, $J_{12}^{(2)}$, $J_{21}^{(1)}$, and $J_{22}^{(2)}$; the latter $J_{11}^{(2)}$, $J_{12}^{(1)}$, $J_{21}^{(2)}$, and $J_{22}^{(1)}$. The integration contours for the integrals of the first and second set are shown in the Fig. 2, *a*, *b*, respectively.

Calculation of the residues at the poles and integration along the cut reveals that the fastest growing terms correspond to the input of residues at the poles of the first-set integrals. Taking into account (63), we get finally for the F_{ij} in (55), (56):

$$F_{11} \sim \exp\left\{(2\xi k - \eta)t\right\}, \tag{65}$$
$$F_{12} \sim \exp\left\{-(2\xi + k) + (2\xi k - \eta)t\right\}, \tag{66}$$
$$F_{21} \sim \exp\left\{-k + (2\xi k - \eta)t\right\}, \tag{67}$$
$$F_{22} \sim \exp\left\{-2(\xi + k) + (2\xi k - \eta)t\right\}. \tag{68}$$

The margin of stability for γ_i in (55), (56) is $\eta = 2\xi k$. In terms of the Fourier modes of the boundaries' perturbations $\overline{\varphi}_i$, $i = 1, 2$, see (28), this means the increment $2\xi k$ for the k-th mode at both boundaries, *i.e.*

$$\overline{\varphi}_1(k,t) = \tilde{F}_{11}\overline{\varphi}_1(k,0) + \tilde{F}_{12}\overline{\varphi}_2(k,0), \tag{69}$$
$$\overline{\varphi}_2(k,t) = \tilde{F}_{21}\overline{\varphi}_1(k,0) + \tilde{F}_{22}\overline{\varphi}_2(k,0), \tag{70}$$

where

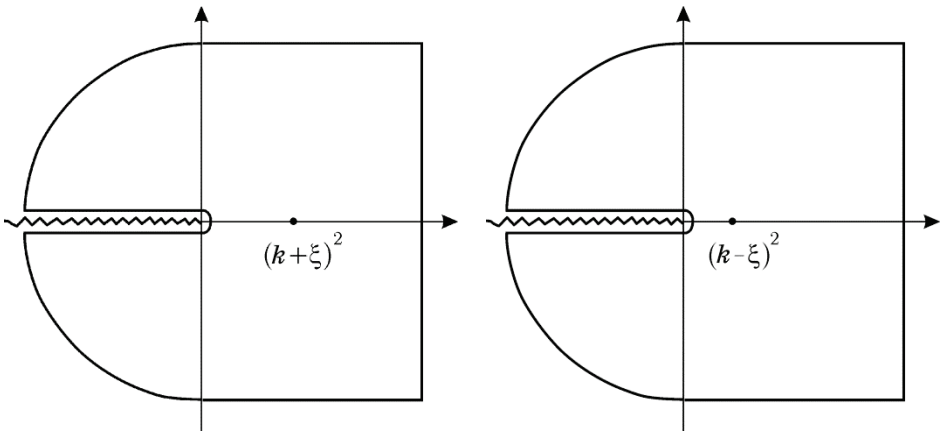

Fig. 2. Integration contours for $J_{11}^{(1)}, J_{12}^{(2)}, J_{21}^{(1)}, J_{22}^{(2)}$ in the complex plane y. Only position of the poles with maximal real part is shown (a). Integration contours for $J_{11}^{(2)}, J_{12}^{(1)}, J_{21}^{(2)}, J_{22}^{(1)}$ in the complex plane y. Only position of the poles with maximal real part is shown (b).

$$\tilde{F}_{11} \sim \exp(2\xi kt), \tag{71}$$

$$\tilde{F}_{12} \sim \exp\{-(2\xi + k) + 2\xi kt\}, \tag{72}$$

$$\tilde{F}_{21} \sim \exp\{-k + 2\xi kt\}, \tag{73}$$

$$\tilde{F}_{22} \sim \exp\{-2(\xi + k) + 2\xi kt\}. \tag{74}$$

Equations (71)–(74) seemingly demonstrate the instability of both boundaries, *i.e.* the exponential growth in time with the increment $2\xi k$ (see also the remark at the beginning of Section 2). Indeed, the perturbations of the boundaries are governed by a linear system; a linear system could be either stable or unstable as a whole; so both boundaries with necessity should be formally either stable or unstable if their interaction is taken into account. However, comparing (71)–(74) it is easily seen that the ratio of the perturbation amplitudes at the oxidizing side to that at the reducing side, $\tilde{F}_{21}/\tilde{F}_{11}$ and $\tilde{F}_{22}/\tilde{F}_{11}$ decreases exponentially with the wave number k. This means that the boundary at the oxidizing side is stable for perturbations with wavelengths smaller than the width of the layer, *i.e.* it is practically morphologically stable, which is in complete agreement with both theoretical considerations and experimental observations in [9]. We would like to point out that this result for the linear stability of the boundaries (for zero surface tension) is exact. The diffusional interaction of the boundaries is taken into account; till now we have not used any additional assumptions. The study of the morphological stability of boundaries for the station-

ary solution is thereby reduced to exploration of the singular points (in the complex plane) of the corresponding integrands.

4. QUASI-STATIONARY APPROXIMATION

While being exact, the approach used in the previous Section is quite complicated. So, it appears reasonable to check the simpler but approximate way of solution of the same problem, compare the results, and then use the simpler approach to solve the essentially more complicated problem for the multiple-layer system. The approximate approach is based on the physical fact that the deviations from the stoichiometry at the boundaries are quite small, $\delta_1 < \delta_2 << 1$; then ξ is a small parameter too

$$\xi = \frac{1}{2} \ln \frac{1-\delta_1}{1-\delta_2} << 1. \tag{75}$$

This means that the characteristic time for the development of the instability $1/2\xi k$, see (65) is large as compared to the characteristic time of the diffusional relaxation inside the layer (which we have taken as a time scale, see Section 2). Then we can use the quasi-stationary approximation for (29), that is, drop the time derivative:

$$2\xi \frac{\partial w}{\partial z} + \frac{\partial^2 w}{\partial z^2} - (k^2 + \eta) w = 0. \tag{76}$$

In this approximation the time evolution enters *via* the boundary conditions (32), (33), see below. We still consider the zero surface tension case, $\Gamma_1 = \Gamma_2 = 0$; the boundary conditions (30), (31) become

$$w\big|_{z=0} + 2\xi(1-\delta_1)\gamma_1(k,t) = 0, \tag{77}$$

$$w\big|_{z=1} + 2\xi(1-\delta_2)\gamma_2(k,t) = 0. \tag{78}$$

The solution of the quasistationary problem is given in Appendix 4; here we only outline the procedure and give the result. First, the solution of (76) satisfying the boundary conditions (77), (78) is obtained. Then it is substituted into the boundary conditions (32), (33); in this way we obtain the system of two ordinary linear equations ((105), (106) in Appendix 4) governing the time evolution of the boundary perturbations $\gamma_1(k, t)$ and $\gamma_2(k, t)$. Solving this system in a standard way, considering k larger than one (see (114), (115)), and returning to the Fourier modes of the boundaries' perturbations $\overline{\varphi}_1(k,t)$ and $\overline{\varphi}_2(k,t)$, yields the following expressions for their time evolution

$$\overline{\varphi}_1(k,t) = A_1 \exp(2\xi k t), \tag{79}$$

$$
\begin{aligned}
A_1 &\simeq \bar{\varphi}_1(0,k) - \exp(-2\xi - k)\bar{\varphi}_2(0,k),\\
\bar{\varphi}_2(k,t) &= B_1 \exp(2\xi k t),\\
B_1 &\simeq \exp(-k)\bar{\varphi}_1(k,0) - \exp\left(-2(\xi + k)\right)\bar{\varphi}_2(k,0),
\end{aligned}
\tag{80}
$$

which coincides with the exact results of the previous section, Eqs. (69)–(74), *i.e.* the approximate analysis of morphological stability based on the quasi-stationary solution yields essentially the same results as the exact approach (for the perturbations with the wave length smaller than the width of the layer). It is worth mentioning that for a single boundary the quasi-stationary approach is exactly equivalent to the method used in [9].

5. SUMMARY AND CONCLUSIONS

In this paper, we have studied the coupled morphological stability of multiple phase boundaries for oxides that are exposed to an oxygen potential gradient. For a single oxide layer this problem was first considered in [9], both experimentally and theoretically. It was shown that the oxidizing boundary is morphologically stable, while the reducing boundary becomes unstable. In the present work the problem of [9] is generalized in an important way: in exploring the morphological stability of two solid/gas interfaces their diffusional interaction is taken into account. To explore the stability of diffusionally interacting boundaries the method developed in [10, 11] is applied. Based on integral transformation of a special kind this method reveals the evolution of the boundaries' perturbations without solving the diffusional problem inside the layer. The study of the morphological stability of boundaries for the stationary solution is thereby reduced to exploration of the singular points (in the complex plane) of the corresponding integrands.

As it was mentioned above, from the formal point the result of [9] may look paradoxical: if the interaction of the boundaries is taken into account the perturbations of the boundaries are governed by a coupled linear system; a linear system could be either stable, or unstable as a whole; so formally both boundaries with necessity should be either stable or unstable. However, comparing (65)–(68) it is easily seen that the ratio of the perturbation amplitudes at the oxidizing side to that at the reducing side decreases exponentially with the wave number k. This means that the boundary at the oxidizing side is practically morphologically stable indeed, which is in complete agreement with both theoretical consideration and experimental observations in [9]. To visualize the mutual influence of the boundaries' perturbations it is practical to plot the $\ln\left|\tilde{F}_{ij} / \tilde{F}_{11}\right|$ (see (65)–(68)) against the wave number k (see Fig. 3).

Because $\xi << 1$, the 'cross-influences' of the perturbations of reducing and oxidizing boundaries $\tilde{F}_{12} / \tilde{F}_{11}$ and $\tilde{F}_{21} / \tilde{F}_{11}$ exhibit identical asymptotical behaviour in k, while the 'self-influence' of the oxidizing boundary $\tilde{F}_{22} / \tilde{F}_{11}$ decreases as $-2k$. It is remarkable that these results for the linear stability of the boundaries of a single layer are not dependent on the width of the stationary layer and (for zero surface tension) are exact. On the other hand, while being exact, the above approach is quite complicated. So, our strategy was to check the simpler but approximate way of solution of the same (single-layer) problem, compare the results, and then use the simpler approach to solve the essentially more complicated problem for the multi-layer system. The approximate approach is based on the physical fact that the deviations from the stoichiometry at the boundaries are quite small and, consequently, ξ (see Eq. (75)) is a small parameter. This means that the characteristic time for the development of the instability $(2\xi k)^{-1}$ is large as compared to the characteristic time of the diffusional relaxation inside the layer (which we have taken as a time scale, see Section 2). Therefore the quasi-stationary approximation is justified, the approximate analysis of morphological stability based on the quasi-stationary solution yields essentially the same results as the exact approach. It is worth mentioning that for a single boundary the quasi-stationary approach is exactly equivalent to the method used in [9]. Now it is evident that for a multi-layer system the ratio of characteristic times will not change

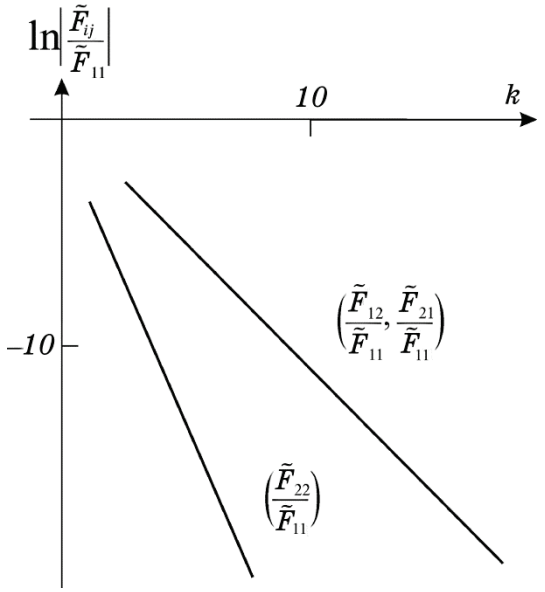

Fig. 3. Plot of $\ln\left|\tilde{F}_{ij} / \tilde{F}_{11}\right|$ against the wave number k for the case of a single layer.

qualitatively (if the diffusion coefficients in the layers are not too different), so, application of the much simpler approximate method is again justified; this problem will be studied in the Part 2 of this paper.

ACKNOWLEDGEMENT

We acknowledge the help of Dr. L. Davydov in preparing the Figures.

APPENDIX 1

If we look for the stationary ('zero order') solution, the equations (2) and (5)–(8), are reduced to [9]

$$-V\frac{dC_s}{dZ} - D\frac{d^2C_s}{dZ^2} = 0, \tag{81}$$

$$C_s\big|_{Z=0} = C_1 = \frac{\delta_1}{\omega},\ C_s\big|_{Z=L} = C_2 = \frac{\delta_2}{\omega}, \tag{82}$$

$$V = \frac{\omega D}{1-\delta_1}\frac{dC_s}{dZ}\bigg|_0 = \tag{83}$$

$$= \frac{\omega D}{1-\delta_2}\frac{dC_s}{dZ}\bigg|_L. \tag{84}$$

The solution of (81) satisfying the boundary conditions (82) is [9]:

$$C_s = \frac{C_2 - C_1\exp(-VL/D) - (C_2 - C_1)\exp(-VZ/D)}{1-\exp(-VL/D)}. \tag{85}$$

Now we have two more equations, (83) and (84), to determine V and the stationary width L. Substitution of (85) for C into (83), (84) yields:

$$1-\delta_1 = \omega\frac{C_2 - C_1}{1-\exp(-VL/D)}, \tag{86}$$

$$1-\delta_2 = \omega\frac{C_2 - C_1}{1-\exp(-VL/D)}\exp(-VL/D). \tag{87}$$

It follows from (86), (87):

$$\exp\left(\frac{VL}{D}\right) = \frac{1-\delta_1}{1-\delta_2}. \tag{88}$$

The interesting feature of the present solution is that only the product of V and L is determined by (88), but not each of these quantities sepa-

rately (this reminds on the well-known 'velocity selection controversy' [12]). However, in the present case we have an additional physically motivated condition: the total amount of A atoms is conserved, that is [9]

$$\int_0^{L_0} dZ \frac{1-\delta_0}{\omega} = \int_0^{L} dZ \left(\frac{1}{\omega} - C_s(Z) \right), \tag{89}$$

where L_0 is the initial oxide layer thickness. Substitution of $C_s(Z)$, see (85), into the latter equation yields finally [9]:

$$L = L_0 \frac{\dfrac{1}{\omega} - C_0}{C_2 - C_1} \ln \frac{1 - C_1\omega}{1 - C_2\omega} \tag{90}$$

and

$$V = \frac{D}{L_0} \frac{C_2 - C_1}{\dfrac{1}{\omega} - C_0} = \frac{D}{L_0} \frac{\delta_2 - \delta_1}{1 - \delta_0}. \tag{91}$$

One can easily check that in the limit $(C_2 - C_1) \to 0$ (and, correspondingly, $V \to 0$) the stationary width L approaches the initial width L_0.

For the subsequent stability analysis we will need to know the values of the derivatives $\dfrac{\partial C_s}{\partial Z}$ and $\dfrac{\partial^2 C_s}{\partial Z^2}$ at the boundaries $Z = 0$ and $Z = L$:

$$\left.\frac{\partial C_s}{\partial Z}\right|_{Z=0} = \frac{V}{D}\frac{1-\delta_1}{\omega}, \quad \left.\frac{\partial^2 C_s}{\partial Z^2}\right|_{Z=0} = -\left(\frac{V}{D}\right)^2 \frac{1-\delta_1}{\omega}, \tag{92}$$

$$\left.\frac{\partial C_s}{\partial Z}\right|_{Z=L} = \frac{V}{D}\frac{1-\delta_2}{\omega}, \quad \left.\frac{\partial^2 C_s}{\partial Z^2}\right|_{Z=L} = -\left(\frac{V}{D}\right)^2 \frac{1-\delta_2}{\omega}. \tag{93}$$

APPENDIX 2

Here we give eight complex integrals $J_{lr}^{(m)}$, introduced in equation (63):

$$J_{11}^{(1)} = \int_{a-i\infty}^{a+i\infty} \frac{(\sqrt{y} + \xi + k)\exp(yt)}{\left(1 - \exp(-2\sqrt{y})\right)\left(y - (k+\xi)^2\right)\left(\sqrt{y} - \xi + k\right)} dy, \tag{94}$$

$$J_{11}^{(2)} = \int_{a-i\infty}^{a+i\infty} \frac{(\sqrt{y} + k - \xi)\exp(yt - 2\sqrt{y})}{\left(1 - \exp(-2\sqrt{y})\right)\left(y - (k-\xi)^2\right)\left(\sqrt{y} + \xi + k\right)} dy, \tag{95}$$

$$J_{12}^{(1)} = \int_{a-i\infty}^{a+i\infty} \frac{(\sqrt{y}+\xi+k)\exp(yt-\xi-\sqrt{y})}{\left(1-\exp(-2\sqrt{y})\right)\left(y-(k+\xi)^2\right)\left(\sqrt{y}-\xi+k\right)}\,dy, \tag{96}$$

$$J_{12}^{(2)} = \int_{a-i\infty}^{a+i\infty} \frac{(\sqrt{y}+\xi+k)\exp(yt-\xi-\sqrt{y})}{\left(1-\exp(-2\sqrt{y})\right)\left(y-(k+\xi)^2\right)\left(\sqrt{y}-\xi+k\right)}\,dy, \tag{97}$$

$$J_{21}^{(1)} = \int_{a-i\infty}^{a+i\infty} \frac{(\sqrt{y}+\xi+k)\exp(yt+\xi-\sqrt{y})}{\left(1-\exp(-2\sqrt{y})\right)\left(y-(k+\xi)^2\right)\left(\sqrt{y}-\xi+k\right)}\,dy, \tag{98}$$

$$J_{21}^{(2)} = \int_{a-i\infty}^{a+i\infty} \frac{(\sqrt{y}+k-\xi)\exp(yt+\xi-\sqrt{y})}{\left(1-\exp(-2\sqrt{y})\right)\left(y-(k-\xi)^2\right)\left(\sqrt{y}+\xi+k\right)}\,dy, \tag{99}$$

$$J_{22}^{(1)} = \int_{a-i\infty}^{a+i\infty} \frac{(\sqrt{y}+k-\xi)\exp(yt)}{\left(1-\exp(-2\sqrt{y})\right)\left(y-(k-\xi)^2\right)\left(\sqrt{y}+\xi+k\right)}\,dy, \tag{100}$$

$$J_{22}^{(2)} = \int_{a-i\infty}^{a+i\infty} \frac{(\sqrt{y}+\xi+k)\exp(yt-2\sqrt{y})}{\left(1-\exp(-2\sqrt{y})\right)\left(y-(k+\xi)^2\right)\left(\sqrt{y}-\xi+k\right)}\,dy. \tag{101}$$

APPENDIX 3

The solution of (76) satisfying the boundary conditions (77), (78) is easily obtained:

$$w = \frac{2\xi}{\exp(\lambda_1)-\exp(\lambda_2)}\left\{\left[(1-\delta_1)\exp(\lambda_2)\gamma_1 - (1-\delta_2)\gamma_2\right]\exp(\lambda_1 z) + \right.$$
$$\left. + \left[(1-\delta_2)\gamma_2 - (1-\delta_1)\exp(\lambda_1)\gamma_1\right]\exp(\lambda_2 z)\right\}, \tag{102}$$

where $\lambda_1 = -\xi+\zeta$, $\lambda_2 = -\xi-\zeta$, and $\zeta = \sqrt{\xi^2+k^2+\eta}$. Below we need $\left.\frac{\partial w}{\partial z}\right|_{z=0}$ and $\left.\frac{\partial w}{\partial z}\right|_{z=1}$ only, that is the values of derivatives at the boundaries:

$$\frac{1}{1-\delta_1}\left.\frac{\partial w}{\partial z}\right|_{z=0} = 2\xi\left[(\xi+\zeta\coth\zeta)\gamma_1 - \frac{\zeta\exp(-\xi)}{\sinh\zeta}\gamma_2\right], \tag{103}$$

$$\frac{1}{1-\delta_2}\left.\frac{\partial w}{\partial z}\right|_{z=1} = 2\xi\left[(\xi-\zeta\coth\zeta)\gamma_2 + \frac{\zeta\exp(\xi)}{\sinh\zeta}\gamma_1\right]. \tag{104}$$

Substituting these values into (32), (33) we obtain a system of two equations for $\gamma_1(k, t)$, $\gamma_2(k, t)$:

$$\frac{\partial \gamma_1}{\partial t} = \left[2\xi\zeta \coth \zeta - 2\xi^2 - \eta\right]\gamma_1 - \frac{2\xi\zeta}{\sinh \zeta}\exp(-\xi)\gamma_2, \tag{105}$$

$$\frac{\partial \gamma_2}{\partial t} = \frac{2\xi\zeta}{\sinh \zeta}\exp(\xi)\gamma_1 - \left[2\xi\zeta \coth \zeta + 2\xi^2 + \eta\right]\gamma_2. \tag{106}$$

The solution of this system is obtained in a standard way: substitution of $\gamma_1 = A\exp(\sigma t)$, $\gamma_2 = A\exp(\sigma t)$ yields a linear homogeneous algebraic system for A, B

$$\left[2\xi\zeta \coth \zeta - 2\xi^2 - \eta - \sigma\right]A - \frac{2\xi\zeta}{\sinh \zeta}\exp(-\xi)B = 0, \tag{107}$$

$$\frac{2\xi\zeta}{\sinh \zeta}\exp(\xi)A - \left[2\xi\zeta \coth \zeta + 2\xi^2 + \eta + \sigma\right]B = 0. \tag{108}$$

For solutions of this system to exist the determinant of this system should equal zero, which yields after some algebra the quadratic equation for σ. The roots of the latter equation are

$$\sigma_{1,2} = -(2\xi^2 + \eta) \pm 2\xi\zeta. \tag{109}$$

The solution of the system (105), (106) is

$$\gamma_1 = A_1\exp(\sigma_1 t) + A_2\exp(\sigma_2 t), \tag{110}$$

$$\gamma_2 = B_1\exp(\sigma_1 t) + B_2\exp(\sigma_2 t), \tag{111}$$

where A_i, B_i are calculated in a standard way using initial values $\gamma_i(0, k)$. The margin of stability for γ_i corresponds to zero value of the maximal (positive) root (109), which in its turn means $\eta = 2\xi k$. Again, in terms of the Fourier modes of the boundaries' perturbations $\overline{\varphi}_i$, $i = 1, 2$ this means the increment $\eta = 2\xi k$ for the k-th mode. Correspondingly, to compare the amplitudes at the onset of instability we need only A_1 and B_1

$$A_1 = \frac{1}{2}\left[1 + \coth(\xi + k)\right]\gamma_1(0, k) - \frac{\exp(-\xi)}{2\sinh(\xi + k)}\gamma_2(0, k), \tag{112}$$

$$B_1 = \frac{\exp(\xi)}{2\sinh(\xi + k)}\gamma_1(0, k) + \frac{1}{2}\left[1 - \coth(\xi + k)\right]\gamma_2(0, k). \tag{113}$$

Now, $k = 0$ means the shift of the layer as a whole, for $k \sim 1$ the ('transverse') scale of the perturbation is comparable to the width of the lay-

er, which makes the use of quasistationary approximation problematical. On the other hand, for $\xi + k >> 1$

$$A_1 \simeq \gamma_1(0,k) - \exp(-2\xi - k)\gamma_2(0,k), \tag{114}$$

$$B_1 \simeq \exp(-k)\gamma_1(0,k) - \exp(-2(\xi + k))\gamma_2(0,k), \tag{115}$$

which coincides with the exact results of the Section 3 (k is in the argument of the exponent, so even when it equals 3 or 4 it is quite a reasonable approximation).

REFERENCES

1. G. H. Meier, *Oxidation of Intermetallics* (Eds. H. J. Grabke and M. Schütze) (Weinheim: Wiley-VCH: 1997), p. 15.
2. U. Koops, D. Hesse, and M. Martin, *J. Mater. Res.*, **17**: 2489 (2002).
3. E. Ryshkewitch and D. W. Richerson, *Oxide Ceramics* (Orlando: Academic: 1985).
4. A. Hammou and J. Guindet, *The CRC Handbook of Solid State Electrochemistry* (Eds. P. J. Gellings and H. J. M. Bouwmeester) (Boca Raton: CRC Press: 1996), p. 407.
5. H. J. M. Bouwmeester and A. J. Burggraaf, *The CRC Handbook of Solid State Electrochemistry* (Eds. P. J. Gellings and H. J. M. Bouwmeester) (Boca Raton: CRC Press: 1996), p. 481.
6. M. Martin, *Pure Appl. Chem.*, **75**: 889 (2003).
7. R. Waser, R. Dittmann, G. Staikov, and K. Szot, *Adv. Mater.*, **21**: 2632 (2009).
8. Y. Aoki, C. Wiemann, V. Feyer, H.-S. Kim, C. M. Schneider, H.-S. Yoo, and M. Martin, *Nat. Commun.*, **5**: 3473 (2014).
9. M. Martin and H. Schmalzried, *Ber. Bunsenges. Phys. Chem.*, **89**: 124 (1985).
10. P. O. Mchedlov-Petrossyan, *Reports of the National Academy of Sciences of Ukraine (Doklady NAN Ukrainy)*, No. 1: 78 (2002).
11. P. O. Mchedlov-Petrossyan, *Metallofiz. Noveishie Tekhnol.*, **24**: 25 (2002).
12. J. S. Langer, *Rev. Modern Phys.*, **52**: 1 (1980).
13. O. M. Chekmareva, *J. Techn. Phys.*, **XLI**: 1115 (1971) (in Russian).
14. J. S. Langer, *Acta Metalurgica*, **25**: 1113 (1977).